

DFT probe and visualization of the mechanisms of BF_3 -catalyzed cationic oligomerization of olefins

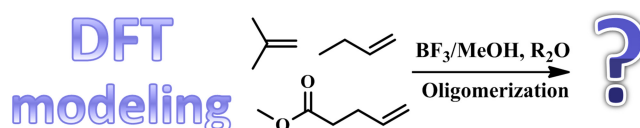
Pavel V. Ivchenko,^{*a,b} Dmitry A. Pyatakov,^a Alexander N. Tavtorkin^a and Ilya E. Nifant'ev^{a,b}

^a A. V. Topchiev Institute of Petrochemical Synthesis, Russian Academy of Sciences, 119991 Moscow, Russian Federation. E-mail: phpasha1@yandex.ru

^b Department of Chemistry, M. V. Lomonosov Moscow State University, 119991 Moscow, Russian Federation

DOI: 10.71267/mencom.7687

The mechanisms of $\text{BF}_3/\text{Pr}^i\text{OH}$ catalyzed oligomerization of isobutylene, dec-1-ene and methyl undec-10-enoate were analyzed using DFT modeling. The newly developed concept implies the participation of two olefin molecules and complex $(\text{BF}_3 \cdot \text{ROH})_2$ as an initiator, the role of the ether additives is to provide high *exo*-selectivity of isobutylene oligomerization. This concept argues the chain-growth oligomerization with intermediate retention of the cationic center (isobutylene), or H^+ elimination (linear α -olefins) explaining the preferable formation of trimers.



New insights into known and prospective processes

Keywords: BF_3 , carbenium ions, cationic oligomerization, dec-1-ene, DFT, isobutylene, polar vinyl monomers.

Cationic oligomerization of olefins can be initiated by different acidic catalysts, the nature of which depends on the nature of the olefin, a target value of the degree of polymerization (DP_n), and desirable chemical structure of the oligomers. Oligomerizations of isobutylene **1** and dec-1-ene **2** occupy a special place among industrially implemented processes, both being based on the use of BF_3/ROH catalyst. However, olefins **1** and **2** would form different products (Scheme 1), namely, highly reactive polyisobutylenes **P1** (along with isomeric **P'1**) with DP_n of ~10–50,¹ and dec-1-ene oligomers **P2** with a high trimer content.^{2,3} Despite the practical importance of these processes, their mechanistic studies are fragmentary and at times contradictory.

For oligomerization of **1**, DFT simulations in the frameworks of the simplest cationic model⁴ allowed one to explain the formation of skeletal isomers and chain scission products. The preference in the formation of *exo*-olefinic product in comparison with oligomers containing internal C=C bond was explained in terms of the relative stability of these species, which is clearly not enough to account for experimentally observed selectivity. In works on DFT modeling of the isobutylene polymerization initiated by $[\text{GaAr}_2]^+$,⁵ $(\text{AlCl}_3)_2\text{H}_2\text{O}$,⁶ sulfated polymers,⁷

CuAlCl_4 ,⁸ and sulfated metal–organic frameworks,⁹ the formation of methyldiene end-groups found an explanation in some cases, but BF_3/ROH catalyzed reaction remained unexplored to date from the theoretical point of view, except the recent work in which a doubtful attempt was made to model the direct interaction of isobutylene **1** with BF_3OH_2 with a formation of $[\text{Bu}^i]^+[\text{BF}_3\text{OH}]^-$.¹⁰ The analysis of the mechanism of dec-1-ene **2** oligomerization usually came down to the simplest cationic model involving the Shubkin mechanism of the isomerization,¹¹ the specific role of the BF_3/ROH catalytic system also remained offscreen (except the only study,¹² whose results are mentioned below).

Recently, oligomerization of polar vinyl monomers of the formula $\text{X}(\text{CH}_2)_n\text{CH}=\text{CH}_2$ ($\text{X} = \text{CH}_2\text{OH}, \text{CO}_2\text{R}, \text{CO}_2\text{H}$; $n = 7, 8$), products of modern oleochemistry,^{13–15} has also caught the attention. The foremost objective of our study was the comparison of isobutylene **1**, linear α -olefin **2**, and polar vinyl monomer such as methyl undec-10-enoate **3** in BF_3/ROH catalyzed oligomerization.

The results of the studies of BF_3/ROH catalyzed dec-1-ene **2** oligomerization are presented in a number of generally recognized works,^{2,3,11,12} whereas the studies of BF_3/ROH catalyzed polymerization of isobutylene **1** are mostly presented in the patent literature,^{16,17} with few exceptions, *e.g.* published study.¹⁸ Oligomerization of polar vinyl monomers like ω -unsaturated esters remains unexplored. To form the experimental basis for DFT modeling, we conducted a series of experiments on $\text{BF}_3/\text{Pr}^i\text{OH}$ catalyzed reactions of olefins **1–3**. As can be seen from the data presented in Table 1, isobutylene **1** formed low-MW oligomers when $\text{BF}_3/\text{Pr}^i\text{OH}$ was less than 1 equiv. (entries 1, 2), addition of Pr_2O decreased DP_n and increased the content of $>\text{C}=\text{CH}_2$ end groups (entry 4). Replacement of Pr_2O by Et_2O resulted in decrease of the catalytic activity (entry 11) while THF deactivated the catalyst (entry 12).

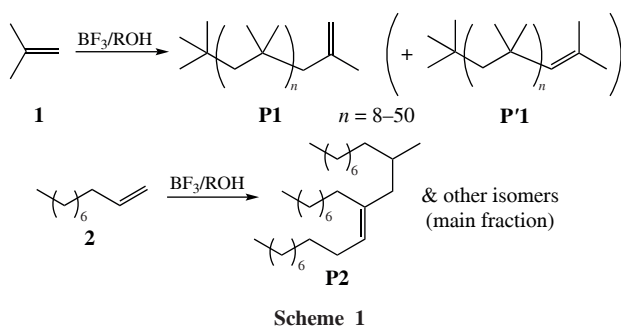
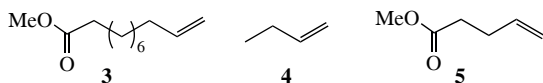


Table 1 Olefin oligomerization results.^a

Entry	Monomer	[BF ₃]/mM	Pr ⁱ OH (equiv.) ^b	Ether ^{b,c}	T/°C	t/min	Conversion (%)	DP _n	D _M	>C=CH ₂ (%) ^d
1	1	5	1	–	–15	120	97	62	2.2	72.2
2	1	5	0.8	–	–15	120	>99	79	3.0	66.9
3	1	5	1.5	–	–15	120	98	43	2.4	86.3
4	1	5	1.5	Pr ₂ O	–15	120	73	28	1.9	89.8
5	1	10	1.5	–	–20	30	97	44	2.4	86.0
6	1	10	1.5	Pr ₂ O	–20	30	86	41	2.0	91.0
7	1	20	1.5	–	–20	30	96	38	2.4	82.4
8	1	20	1.5	Pr ₂ O	–20	30	84	30	2.0	92.8
9	1	30	1.5	–	–15	30	99	17	2.4	76.5
10	1	30	1.5	Pr ₂ O	–15	30	98	16	2.1	87.4
11	1	20	1.5	Et ₂ O	–20	30	22	16	1.5	92.2
12	1	20	1.5	THF	–20	30	6	–	–	–
13	2	50	1	–	30	120	12	2.5	–	–
14	2	50	0.8	–	30	120	92	3.4	–	–
15	3	50	0.8	–	30	120	0	–	–	–

^aBF₃·PrⁱOH and ether were injected to monomer in closed reactor with stirring. ^bMolar equivalents relative to BF₃. ^cWith 0.5 molar equivalents relative to BF₃. ^dMethylidene content in chain ends in cases of isobutylene oligomers (¹H NMR).

Towards dec-1-ene **2**, 1:1 BF₃/PrⁱOH system was virtually inactive (entry 13), and oligomerization was successfully performed with the use of published method based on the catalyst with high BF₃/PrⁱOH ratio (entry 14).² However, under these conditions methyl undec-10-enoate **3** turned out to be completely inert (entry 15).



Boron trifluoride BF₃, MeOH, isobutylene **1**, but-1-ene **4**, model unsaturated ester, methyl pent-4-enoate **5**, and different ethers were selected for DFT simulations using PRIRODA-06 program (*T* = 298.15 K, gas phase, PBE functional, 3 ζ basis set).¹⁹ First, we analyzed the interaction between BF₃ and MeOH, since it is BF₃·ROH complexes that are viewed as a proton sources during the formation of carbenium ions.^{2,12} We found that the formation of (BF₃·MeOH)₂ is energetically preferable (–10.6 kcal mol^{–1} in *G* scale), the dimer is formed by two intermolecular hydrogen bonds [*d*(OH···F) = 1.599 Å] and represents 8-membered cycle (see Online Supplementary Materials). Interactions of BF₃·MeOH and (BF₃·MeOH)₂ with

other possible components of the reaction mixture are of particular interest (Table 2).

The results of these calculations allow us to explain inactivity of undecenoate **3** in BF₃/ROH catalyzed reaction: the activation of the C=C bond simply does not occur due to coordination of the proton at carbonyl oxygen. It should also be noted that THF has the maximum binding enthalpy among other ethers, which contributes to lowering isobutylene polymerization rate in the presence of THF.

The subsequent modeling was performed in order to establish the mechanism of initiation and propagation of oligomerization of butylenes **1**, **4**. At the beginning of our study, we relied on the Wang's results proposing that olefin oligomerization is initiated by BF₃·ROH species.¹² However, our attempts of the scanning along the reaction coordinate for the protonation of **1** under the action of BF₃·MeOH failed. So we decided to look for concerted activation mechanism involving two isobutylene molecules, by analogy with the mechanism proposed previously for dimerization of **1** on sulfated metal-organic frameworks.⁹ However, in the case of BF₃·MeOH the calculated ΔG^\ddagger values exceeded 30 kcal mol^{–1} (see Online Supplementary Materials), which is incompatible with the reaction conditions (–20 °C).

Our experiment (see Table 1, entry 2) showed that faster formation of higher-MW polymer with poor *exo*-selectivity is observed at [BF₃]/[PrⁱOH] > 1. This suggested that under these conditions the process can be initiated by (BF₃)₂·MeOH species. Optimization of the molecular structure of (BF₃)₂·MeOH revealed that this adduct is exergonic (ΔG_f = –14 kcal mol^{–1}) and can protonate isobutylene **1** via low-energy TS (ΔG^\ddagger = 8.1 kcal mol^{–1}) with a formation of the [Me₃C]⁺[(BF₃)₂OMe][–] ion pair. Apparently, similar mechanism of activation occurs under conditions of excess BF₃, but it runs pure cationic oligomerization with a formation of high-MW products and low *exo*-selectivity. We have also tried to simulate oligomerization of but-1-ene **1** using (BF₃)₂·MeOH as an initiator, however, unsuccessfully.

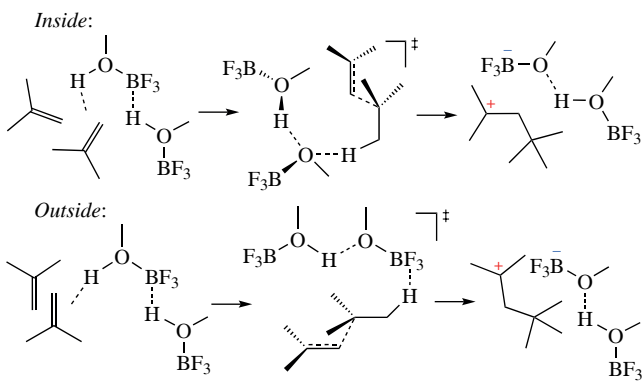
In this way, isobutylene oligomerization of our interest (low-MW oligomers with *exo*-selectivity >90%) should have a different initiator and mechanism. We propose that (BF₃·MeOH)₂ acts as an initiator, and modeled possible variants of concerted mechanism involving BF₃·MeOH dimer and two molecules of **1**, which differ by the arrangement of BF₃·MeOH dimer (Scheme 2). As a result, TS for 'inside' (also known as 'push-pull'²⁰) and 'outside' mechanisms were found.

In a similar way, the step of the reaction of [BuⁱCH₂CMe₂]⁺ with isobutylene **1**, and first two steps of (BF₃·MeOH)₂-initiated

Table 2 The binding affinity of BF₃·MeOH and (BF₃·MeOH)₂ with the model compounds, and selected geometry parameters of the corresponding complexes.^a

Lewis base	Enthalpy of binding/ kcal mol ^{–1} ^b	Distances/Å		
		<i>d</i> (B–O) ^c	<i>d</i> (OH···O) or <i>d</i> (OH···CH ₂ =)	<i>d</i> (OH···CH ₂ ≤)
MeOH	–16.09/–7.34	1.630/1.652	1.555/1.449	
Me ₂ O	–14.52/–7.83	1.631/1.564	1.540/1.465	
Et ₂ O	–15.14/–8.87	1.626/1.559	1.518/1.437	
Pr ₂ O	–15.13/–8.95	1.625/1.557	1.514/1.429	
Pr ₂ O	–15.25/–8.96	1.627/1.562	1.530/1.445	
Bu ⁱ OMe	–15.36/–8.88	1.627/1.560	1.525/1.450	
THF	–16.10/–10.53	1.617/1.554	1.489/1.410	
1	–9.41/–1.68	1.664/1.592	2.012/1.946	2.309/2.270
4	–8.11/–0.50	1.673/1.600	2.108/2.024	2.236/2.148
5 on C=C	–7.71/–0.52	1.676/1.609	2.125/2.080	2.223/2.210
5 on C=O	–14.98/–7.88	1.625/1.571	1.575/1.496	
5 on OMe	–9.02/–1.36	1.659/1.591	1.673/1.608	

^aValues refer to complexes of BF₃·MeOH and (BF₃·MeOH)₂ separated by a slash. ^b $\Delta H = H(\text{complex with } \text{BF}_3\text{-MeOH}) - [H(\text{Lewis base}) + H(\text{BF}_3\text{-MeOH})]$ or $\Delta H = H(\text{complex with } (\text{BF}_3\text{-MeOH})_2) - [H(\text{Lewis base}) + H((\text{BF}_3\text{-MeOH})_2)]$. ^cFor the complexes with (BF₃·MeOH)₂, the lengths of B–O bonds in BF₃·MeOH directly bound with a base are given.



Scheme 2

oligomerization of butene **4** that mimic oligomerization of dec-1-ene **2**, were modeled. Since the processes under study are of the associative nature, the energy profiles of two first steps are presented in Figure 1 in *G* and *H* scales (relative to the sums of *G* and *H* of two olefin and $(BF_3 \cdot MeOH)_2$ molecules). As can be seen in Figure 1, the ‘outside’ initiation and propagation is preferable for **1**, and the activation barrier of the propagation step is lower. For linear **4**, the ‘inside’ pathway seems more favorable in terms of activation barriers, but the adduct formation at the first step is thermodynamically forbidden ($\Delta H > 0$). Both activation barriers for ‘inside’ pathway can be surmounted under the reaction conditions, and at the second step of **4** oligomerization the local minimum at the potential energy surface corresponds to the structure presented in Figure 2 that further relaxes to trimer of **4** and $(BF_3 \cdot MeOH)_2$. And is not this the reason for the selective formation of trimers in BF_3/ROH catalyzed oligomerization of the α -olefins?

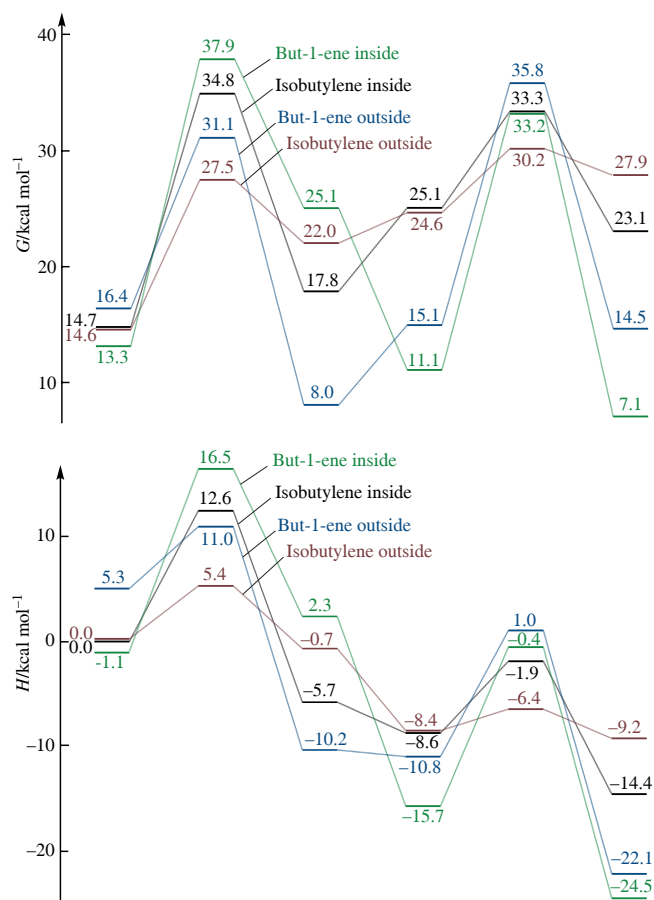


Figure 1 Free energy (top) and enthalpy (bottom) profiles obtained by DFT modeling of the first two steps of oligomerization of isobutylene **1** and but-1-ene **4**, initiated by $(BF_3 \cdot MeOH)_2$.

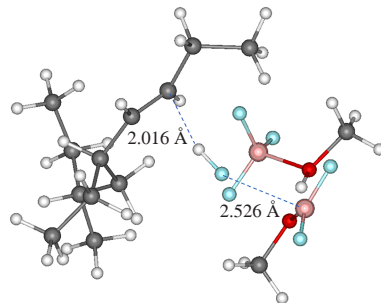


Figure 2 Molecular structure of the reaction intermediate of but-1-ene trimerization that corresponds to the local minimum on the potential energy surface.

On the contrary, isobutylene **1** would oligomerize with a formation of the ion pairs, and when the reaction proceeds *via* the ‘outside’ pathway, tertiary carbocation and counterion are spatially separated. If so, we just need to clarify the role of the ethers in a formation of polyisobutylenes **P1** with high $>C=CH_2$ content. In theory R_2O can interact with tertiary cation with a formation of $[Bu^tCH_2CMe_2-OR_2]^+$ adduct and *via* proton elimination from Me and CH_2 fragments. By the results of the modeling, the adduct formation was exergonic only in the case of THF, therefore, THF may act as a reagent forming the resting state of the cationic polymerization of **1** (see Table 1, entry 12). More significantly, the modeling revealed the clear preference of the formation of *exo*-olefinic bond. This process was barrierless for Me_2O , Et_2O , Pr_2O and Ph_2O ; for Bu^tOMe and THF the free activation energies did not exceed ~ 0.6 kcal mol⁻¹.

To summarize, DFT modeling allowed us to explain some key experimental features of the olefin cationic oligomerization, and the results of mechanistic simulations can be used in further development of the cationic catalysts of this industrially significant process.

This work was supported by The Russian Science Foundation (grant no. 24-43-20016) and performed using the equipment of the Shared Research Center ‘Analytical center of deep oil processing and petrochemistry of TIPS RAS’.

Online Supplementary Materials

Supplementary data associated with this article can be found in the online version at doi: 10.71267/mencom.7687.

References

- Y. Li, M. Cokoja and F. E. Kühn, *Coord. Chem. Rev.*, 2011, **255**, 1541; <https://doi.org/10.1016/j.ccr.2010.12.007>.
- J. A. Brennan, *Ind. Eng. Chem. Prod. Res. Dev.*, 1980, **19**, 2; <https://doi.org/10.1021/i360073a002>.
- A. Onopchenko, B. L. Cupples and A. N. Kresge, *Ind. Eng. Chem. Prod. Res. Dev.*, 1983, **22**, 182; <https://doi.org/10.1021/i300010a006>.
- P. Dimitrov, J. Emert, J. Hua, S. Keki and R. Faust, *Macromolecules*, 2011, **44**, 1831; <https://doi.org/10.1021/ma102645w>.
- M. R. Lichtenhaler, A. Higelin, A. Kraft, S. Hughes, A. Steffani, D. A. Plattner, J. M. Slattery and I. Krossing, *Organometallics*, 2013, **32**, 6725; <https://doi.org/10.1021/om4005516>.
- M. N. Vo, Y. Basdogan, B. S. Derksen, N. Proust, G. A. Cox, C. Kowall, J. A. Keith and J. K. Johnson, *ACS Catal.*, 2018, **8**, 8006; <https://doi.org/10.1021/acscatal.8b01494>.
- Y. Liu, B. Yang and C. Yi, *Ind. Eng. Chem. Res.*, 2013, **52**, 6933; <https://doi.org/10.1021/ie400406j>.
- G. Liu, G. Wu, Y. Liu, R. Hu and G. Gao, *Fuel*, 2022, **310**, 122379; <https://doi.org/10.1016/j.fuel.2021.122379>.
- B. Yang, J. Mendez-Arroyo, C. May, J. Yao and D. H. Ess, *J. Phys. Chem. C*, 2023, **127**, 8539; <https://doi.org/10.1021/acs.jpcc.3c01031>.
- V. A. Babkin, D. S. Andreev, A. V. Ignatov, E. S. Titov, A. I. Rakhimov and N. A. Schreibert, *Fluorine Notes*, 2022, **141** (2), 3; <https://doi.org/10.17677/fn20714807.2022.02.02>.

11 R. L. Shubkin, M. S. Baylerian and A. R. Maler, *Ind. Eng. Chem. Prod. Res. Dev.*, 1980, **19**, 15; <https://doi.org/10.1021/i360073a005>.

12 J. Wang, H. Li, X. Chen, W. Shi, N. Zhang, F. Bai, X. Wang, S. Wang, X. Xu and L. Wang, *Chin. J. Chem. Eng.*, 2019, **27**, 2687; <https://doi.org/10.1016/j.cjche.2019.05.006>.

13 P. V. Ivchenko and I. E. Nifant'ev, *Green Chem.*, 2025, **27**, 41; <https://doi.org/10.1039/d4gc04862h>.

14 W. Yan, Z. You, K. Meng, F. Du, S. Zhang and X. Jin, *Chin. J. Chem. Eng.*, 2022, **48**, 44; <https://doi.org/10.1016/j.cjche.2021.10.008>.

15 S. Singh, S. Sharma, S. J. Sarma and S. K. Brar, *Environ. Prog. Sustainable Energy*, 2023, **42**, e14008; <https://doi.org/10.1002/ep.14008>.

16 H. P. Rath, F. Hoffmann, P. Reuter and H. Mach, *Patent US 5191044 A*, 1993; <https://patents.google.com/patent/US5191044A>.

17 H. P. Rath, U. Kanne and F. van Deyck, *Patent US 6407186B1*, 2002; <https://patents.google.com/patent/US6407186B1>.

18 L.-B. Zhang, Y.-X. Wu, P. Zhou, G.-Y. Wu, W.-T. Yang and D.-S. Yu, *Chin. J. Polym. Sci.*, 2011, **29**, 360; <https://doi.org/10.1007/s10118-011-1042-x>.

19 D. N. Laikov, *Chem. Phys. Lett.*, 1997, **281**, 151; [https://doi.org/10.1016/s0009-2614\(97\)01206-2](https://doi.org/10.1016/s0009-2614(97)01206-2).

20 K. S. Minsker, Yu. A. Sangalov, V. A. Babkin and O. A. Ponomarev, *Theor. Exp. Chem.*, 1985, **20**, 627; <https://doi.org/10.1007/bf00568916>.

Received: 21st November 2024; Com. 24/7687